CRACK DEVELOPMENT ANALYSIS OF AN THIN UHPC ELEMENT

*Michaela Kopálová, **

Katedra betonových a zděných konstrukcí, Fakulta stavební,
České vysoké učení technické v Praze, Thákurova 7/2077, 166 29 Praha 6, Česká republika.
michaela.kopalova@fsv.cvut.cz

ABSTRAKT

UHPC (ultra vysokohodnotný beton) je inovativní materiál, díky kterému je možné realizovat lehčí a konstrukčně optimalizované konstrukce s vysokou životností. V tomto příspěvku je představeno experimentální ověření chování stojin komorového mostu s prefabrikovanými stěnovými panely na zmenšených vzorcích. Předem předpjaté nosníky byly vyhotoveny ve dvou variantách – plnostěnný a s vylehčenou stojinou, která reprezentuje chování prefabrikovaných stěn na mostě. Na základě výsledků experimentu jsou obě varianty porovnány a jsou odvozeny numerické a materiálové modely v programu SCIA Engineer pro UHPC.

KLÍČOVÁ SLOVA

UHPC • Smykové namáhání • Tenkostěnný prvek • Prefabrikace • Předpětí

ABSTRACT

UHPC (Ultra High-Performance Concrete) is an innovative material that enables design of lightweight and structurally optimized, long-lasting structures. In this paper, an experimental analysis of precast webs of a "butterfly web" box-girder bridge on scaled-down specimens is presented. Pretensioned beam specimens were analysed in 2 variants – with continuous web and with lightened web. Based on the experimental results both variants are compared and numerical and material models suitable for UHPC modelling in software SCIA Engineer are presented. In SCIA Engineer the modified Mazarz material damage model is implemented which is applicable for material with residual strength typical for FRC and UHPFRC.

KEYWORDS

UHPC • Thin element • FRC shear resistance • Structural optimization.

1. INTRODUCTION

This paper describes an experimental analysis of initiation and propagation of cracks in webs of a bridge with a box cross-section. The web is composed of thin UHPC precast walls rigidly connected to the bottom and top slab of the bridge cross-section. The shape of these UHPC wall elements was optimized in order to achieve the most favourable stress distribution. The optimal shape was determined from optimisation based on the principal tensile and compressive stress distribution with distinctive shape of the tensile and compressive diagonal, which are caused by shear force transfer between the top and bottom slab. The web of the box cross-section is lightened and suitable for prefabrication so these elements may be used on bridges over 100 m span (concept shown on Figure 1). The design of lightened web elements is based on concepts of so called "butterfly web" bridges [1].

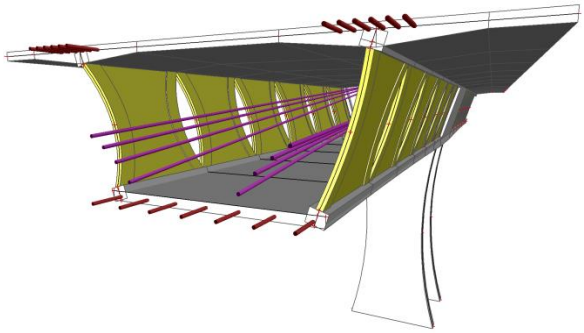

Figure 1: *"Butterfly web bridge" concept visualisation.*

Precast panels connected with top and bottom slab by composite action do not transfer shear force as a continuous web would and their behaviour is well differentiated with tensile and compressive diagonals and is closer to a Warren truss system [2]. Based on the research in this paper, the viable description of the behaviour is the analogy of a Vierendeel beam, where discrete web elements act as vertical members with rigid connection to the top and bottom slab (flange) in the longitudinal direction. Vierendeel frames are more appropriate to describe the behaviour of UHPC webs, due to different UHPC properties in plain tension and tension due to bending.

2. ANALYSIS METHODS IMPLEMENTED IN SCIA ENGINEER FOR UHPFRC ANALYSIS

Physical non-linear analysis represents a very powerful tool for analysing any kind of structure in civil engineering created not only from UHPFRC but also from other materials. Generally, there could be significant differences of results compared to a linear analysis, especially in case of hyper-static

* Školitel: doc. Ing. Štěpán Růžička, Ph.D.

structures. In case of linear analysis, only the E-modulus and Poisson ratio of the material are considered for the preparation of the stiffness matrix. There is no stress redistribution based on increasing the strain in the component. On the other side the non-linear analysis provides a stress redistribution and increase of the bearing capacity after reaching the ultimate strain until the collapse mechanism. This mechanism is based on different values of stress and strain, dependent on a predefined non-linear stress-strain relationship in the material diagram.

Two approaches are usually used for considering fibres in non-linear analysis. The first one uses the fibre and concrete matrix independently. The second and more common one considers the steel fibre directly in the behaviour of the concrete material. The second, more exact option was selected in this paper.

A typical shape of the stress-strain diagram is best described with a parabolic behaviour in compression in the same way as for standard concrete. The tensile behaviour displays a narrow peak expressed by the mean tensile strength. From the point of strain, this peak works very well as a crack localizer. After the crack formation, the toughness of steel reinforced fibre concrete allows to keep a certain level of tensile stress with increasing of the strain up to failure.

2.1. Modified Mazarz material damage model

The nonlinear calculation is based on a very efficient damage material model called the Mazars model 0. This material model is very well applicable for a material diagram with peaks and descending stress-strain diagrams typical for steel fibre concrete. The combination of elasticity and damage behaviour is combined in this material model. Moreover, the damage description was initially considered as isotropic and directly affecting the stiffness matrix. The original Mazars model was updated to the "modified Mazars model" based on [4] which has been derived from [6]. This leads to a very simple anisotropic damage model better respecting different behaviours of the fibre concrete in tension and compression and mainly to the decomposition of the stress tensor ($\boldsymbol{\sigma}$) to the tension ($\boldsymbol{\sigma^t}$) and compression ($\boldsymbol{\sigma^c}$) parts

$$\boldsymbol{\sigma} = \boldsymbol{\sigma^t} + \boldsymbol{\sigma^c} \tag{1}$$

based on principal stresses and using 2nd order tensors $\boldsymbol{e_i}$.

$$\boldsymbol{\sigma} = \sum_{i=1}^{3} \sigma_i \boldsymbol{e_i} \otimes \boldsymbol{e_i} \tag{2}$$

It is suitable to define 4th order projection tensors for tension $\boldsymbol{P^t}$ and compression $\boldsymbol{P^c}$,

$$\sigma^t = P^t : \sigma$$
$$\sigma^c = P^c : \sigma \tag{3}$$

where these tensors are obtained as

$$\boldsymbol{P^t} = \sum_{i=1}^{dim} \langle \sigma_i \rangle (\boldsymbol{e_i} \otimes \boldsymbol{e_i}) \, (\boldsymbol{e_i} \otimes \boldsymbol{e_i})$$
$$\boldsymbol{P^c} = \delta_{ik}\delta_{jl} \boldsymbol{e_i} \otimes \boldsymbol{e_j} \otimes \boldsymbol{e_k} \otimes \boldsymbol{e_l} - \boldsymbol{P^t} \tag{4}$$

The item $\langle * \rangle$ is the MacAuley bracket in the formula above. Additionally, item "dim" corresponds to 2D or 3D dimensional problems.

The resultant stress tensor is based on the so called "effective damage parameter" in tension (d^t) and in compression (d^c) which determines changes of the stiffness depending on the elastic estimation of stress ($\boldsymbol{\sigma^{trial}}$) from the loading.

$$\boldsymbol{\sigma} = (1 - d^t) \cdot \boldsymbol{\sigma^t} + (1 - d^c) \cdot \boldsymbol{\sigma^c} = [(1 - d^t) \cdot \boldsymbol{P^t} + (1 - d^c) \cdot \boldsymbol{P^c}] : \boldsymbol{\sigma^{trial}} \tag{5}$$

This elastic estimation of stress can be expressed using the constitutive tensor (C) as follows:

$$\boldsymbol{\sigma^{trial}} = \boldsymbol{C} : \boldsymbol{\varepsilon} \tag{6}$$

The damage parameters are calculated based on the equivalent Mazars strains (ε_t; ε_c) which help for determining of actual values of stress from the stress-strain diagram of the material.¨

$$d^t = 1 - \frac{\sigma(\varepsilon_t)}{\sigma^{trial}(\varepsilon_t)}; \; d^c = 1 - \frac{\sigma(\varepsilon_c)}{\sigma^{trial}(\varepsilon_c)} \tag{7}$$

As the stress-strain diagram of UHPC typically has a descending branch of stress-strain in tension, it is not possible to use the tangential constitutive tensor ($\boldsymbol{C}$) but it is recommended to use the secant one ($\boldsymbol{C^s}$) to fulfil its positive definition which is finally calculated as below.

$$\boldsymbol{C^s} = [(1 - d^t) \cdot \boldsymbol{P^t} + (1 - d^c) \cdot \boldsymbol{P^c}] : \boldsymbol{C}; \tag{8}$$

Additionally, the effect of cracks must be considered during application. Here an analogy with the thermodynamic variable is applied for the two main damage states which are cracking of concrete in tension and crushing in compression. In case of plotting the surface failure of the steel fibre reinforced concrete the very well-known curve described by Kupfer 0 for biaxial loading is obtained which is also typical for regular reinforced concrete. The standard Newton-Raphson method is used for solving of this physical non-linear problem.

3. EXPERIMENTAL ANALYSIS OF UHPC WEB ELEMENTS

3.1. Description of tested UHPC specimens

For experimental analysis of slender structural members of UHPC under shear loading 2 types of beam specimens were designed – one with a full, continuous web and one with a longitudinally lightened web. These beams have an I-cross-section with sufficiently designed flanges with longitudinal pretensioned tendons in order to mitigate effects of bending. The topology of these beams is apparent on figure 2 below. The aim of this experimental setup is to verify the behaviour of lightened specimens and viability of the application of similar larger scale precast and pretensioned web elements in greater magnitude and on bridges of span over 100 m.

In the structural analysis software SCIA Engineer the specimen was modelled with a loading mechanism as half (from support to midspan) with corresponding boundary conditions in order to reduce the analysis time. Furthermore, the FEM mesh was refined in areas where cracks were expected to develop.

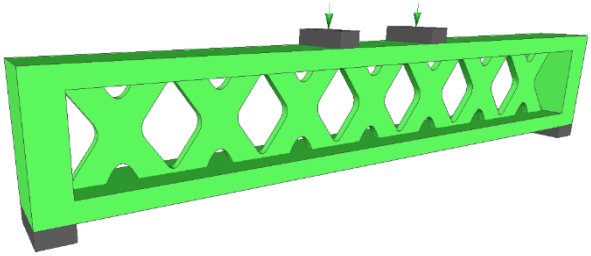

Figure 2:*Visualisation of an UHPC specimen*

3.1. UHPC beam specimens and UHPC mixture characteristics

In total, 6 beam specimens were casted and loaded in 4-point bending tests, 3 specimens with continuous web labelled P1, P2, P3 and 3 beams with lightened web labelled V1, V2, V3. The first beam from each set (P1, V1) was loaded till failure. On the other 2 specimens in each set first a cyclical loading was applied and after that the specimens were loaded till failure. The compressive strength of the UHPC mixture was measured on cubes 100x100x100 mm and the average compressive strength was 157,1 MPa. The tensile strength in bending was measured on prismatic specimens of 40x40x160 mm and was in average 28,0 MPa. The modulus of elasticity was measured on cylindrical specimens 300 mm high with diameter 150 mm and the average modulus of elasticity was 51,6 GPa.

4. RESULTS

In this section the results are presented of the experiment for both types of beam specimens. The results are presented in the form of force – deflection diagrams and are approximated by a numerical model in SCIA Engineer 18 where a non-linear material model with damage was used. Basic characteristics of the material model were set according to experimental results on cubes (strength in compression), prisms (tensile strength in bending) and cylinders (modulus of elasticity). These specimens had the same age in the time of testing as the bigger beam specimens. For both beam specimens the numerical model took into account the effects of longitudinal prestressing with estimated short-term and long-term losses of 15%. The age of the specimens at the time of testing was in average 90 days.

4.1. Results on beam with full web

The beams with continuous web were tested in 4-point bending in 2 separate scenarios. In the first scenario the first beam (P1) was loaded by a continuous increase of displacement till failure. In the second scenario the 2nd and 3rd beams (P2 and P3) were loaded with a cyclic loading pattern. Five loading cycles of approximately 0 – 100 kN were applied and the beams were loaded till failure. The force – displacement diagram of this experiment is presented on figure 3 below.

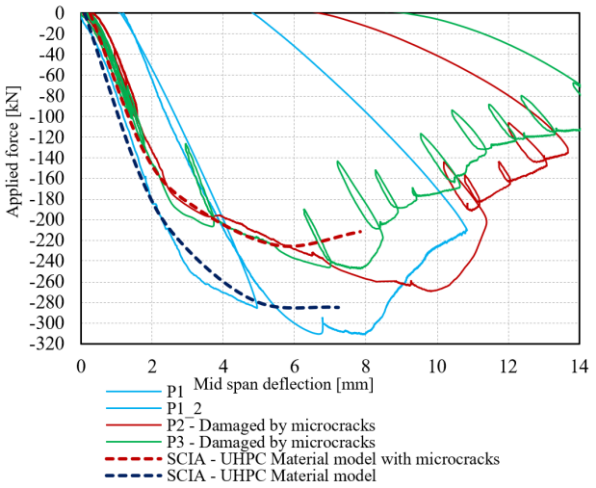

Figure 3: *Force – displacement diagram: beams with continuous webs*

From the force – displacement diagram is apparent the softening of the beams with applied cyclical loading to the magnitude of the applied load of approximately 150 kN when compared to the beam which was loaded without the cyclic scenario. Furthermore, in the specimens with applied cyclical loading the first visible cracks appeared at much lower magnitude of the acting force. Cause of this behaviour is the initiation of microcracks when cyclical loading was applied. From the figure 3 it is apparent, that this effect has a significant effect on both the mean and residual tensile strength of the UHPC.

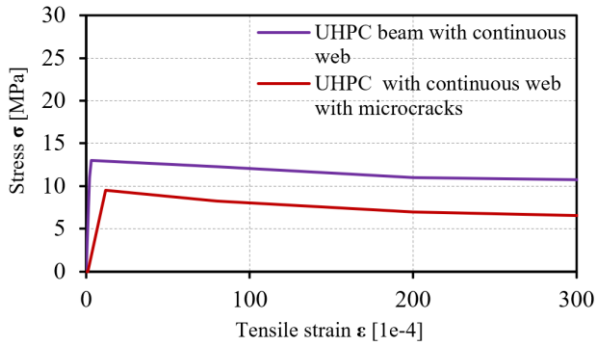

Figure 4: *Stress – strain diagrams of UHPC – tension*

For the numerical model of beams with continuous webs were used material models of UHPC with characteristics shown below in figure 4. Magnitudes of mean and residual stresses were obtained iteratively in order to achieve a behaviour consistent with the measured force – displacement diagram in figure 3. Magnitudes of residual strain in the material model are dependent on the FEM mesh size. In this case the size of the mesh in areas of crack initiation was set to 10 mm and the crack width was limited to 5 mm. This corresponds to the upper limit of residual strain for the mesh elements to be 50% (for better readability of values in figure 4 only the section below 3% strain is displayed).

The type of failure and shape of the developed cracks is apparent on figure 5 below. Photography taken during the experiment is compared to the shape of the developed crack in program SCIA Engineer 18.

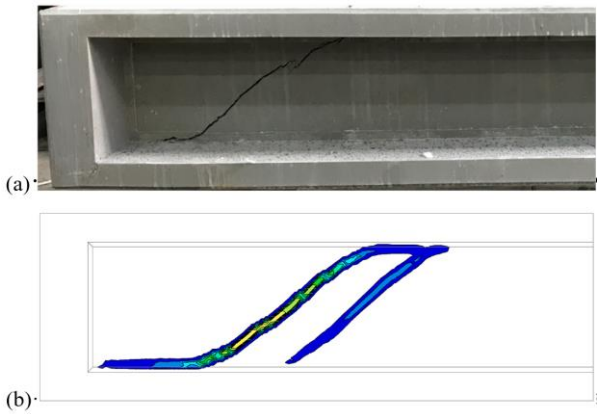

Figure 5: *Analysis of crack shape: photo (a); development of macrocracks (b) in the numerical model*

4.2. Results on beam with lightened web

The beams with lightened web were tested in 4-point bending in 2 separate scenarios the same way as the beams with a continuous web. In the second scenario a cyclic loading pattern was applied on specimens V2 and V3. Five loading cycles of approximately 0 – 40 kN were applied and the beams were loaded till failure. The force – displacement diagram of this experiment is presented on figure 6 below.

From the force – displacement diagram the softening of the beams with applied cyclical loading to magnitude of applied load of approximately 50 kN is apparent when compared to the beam which was loaded without the cyclic scenario. Furthermore, in the specimens with applied cyclical loading the first visible cracks appeared at a significantly lower magnitude of the acting force.

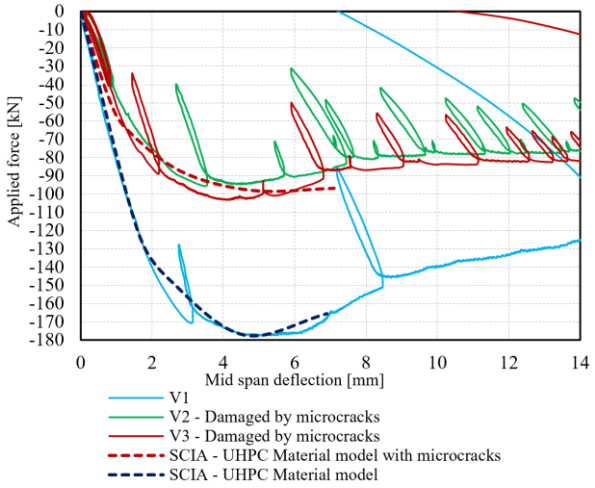

Figure 6: *Force – displacement diagram: beams with lightened webs*

For the specimen which was not cyclically loaded a much better performance can be seen in comparison with the beam which was subjected to cyclical loading. The increase of the load bearing capacity between the scenarios is much greater than in the case of specimens with a continuous web. This effect is very important and is influenced by the fact, that tensile strength of UHPC in tension is several times greater when subjected to bending rather than plain tension. The tension strength in bending was experimentally verified on prismatic specimens 40x40x160 mm, which represents cross-section with comparable dimensions as the thickness of the web of the beam specimens to mitigate the size effect. For the numerical model of beams with lightened webs material models of UHPC were used with characteristics as shown below in figure 7.

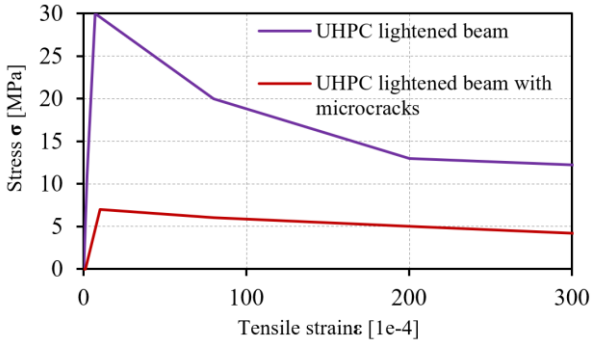

Figure 7: *Stress – strain diagrams of UHPC – tension*

The type of failure and shape of the developed cracks is apparent on figure 8 below and again shows a good correlation between the observed crack distribution and the numerical model.

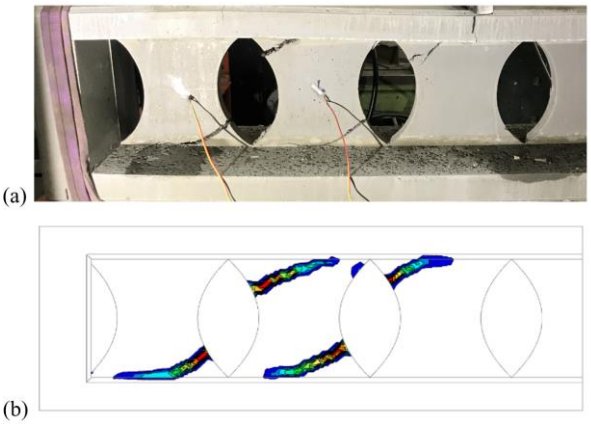

Figure 8: *Analysis of crack shape: photo (a); development (b) of macrocracks in the numerical model*

4.3. Comparison of solid and lightened web beams

For an objective comparison of beams with continuous and lightened webs which were loaded till failure (loading scenario 1) it is prudent to determine the values of the maximal applied loading on such lightened specimens, that would require an identical amount of UHPC as the specimen with a continuous web. Such modified specimen would have a lightened web with thickness 48,4 mm increased by 38%. On figure 9 below the comparison is shown of the magnitude of the applied forces on the level of macrocrack initiation and with a maximal applied load.

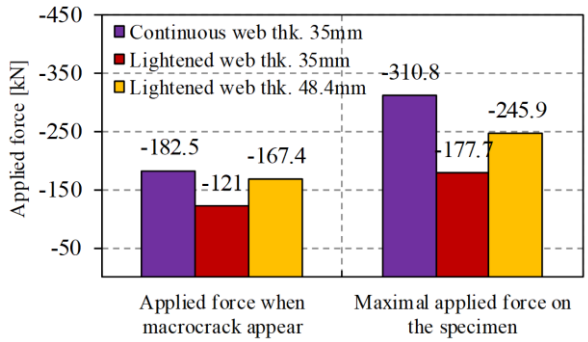

Figure 9: *Comparison of specimen behaviour*

The recorded effect of reduction of both the mean and residual strength of UHPC beam specimens loaded with cyclical loading when compared to a beam loaded straight till failure without cyclical loading is more severe in the case of the lightened specimen. This effect is caused by a higher magnitude of tensile stresses in the specimens when the cyclical loading is applied. In localised areas of the lightened web specimen the magnitudes of tensile stresses rise to 16,5 MPa when compared to the tensile stresses in the specimen with a continuous beam 9,0 MPa. Localised tensile areas in the lightened beam with a greater magnitude lead to higher initiation of microcracks and more severe damage of the specimens, before any macrocracks are visible. On figure 10 below are shown the distributions of the principal tensile stresses from the combination of self-weight, prestressing and the amplitude of the applied cyclical load.

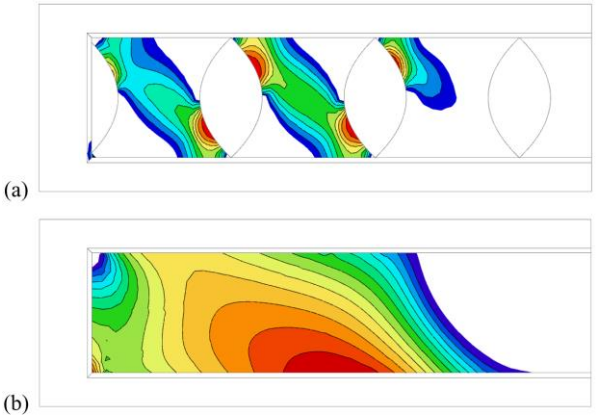

Figure 10: *Maximal tensile stresses in web of (a) lightened beam and (b) beam with continuous web during cycled loading*

5. DISCUSSION

The comparison of a beam with lightened and continuous web is made on specimens with the same amount of material required. The beam with continuous web has a web thickness of 35mm (as the real specimen) and the lightened beam has a recalculated web thickness of 48,4 mm. The first visible macrocracks appear in the case of a beam with lightened web on a load level 15% lower and maximal loading 22% lower than the beam with continuous web. Despite the fact that the magnitudes are lower, there are the following important aspects:

The lightened beam shape may yet be further optimized (increase thickness on edges of the wall segments, where macrocracks first appear).

Possibility of prefabrication of separate web segments to ensure superior quality.

Due to clear and consistent shear force transfer by the web segments, these segments may be provided with prestressing tendons in the direction of the tensile diagonal to mitigate tensile stresses.

Contradictory to analysis performed prior the experiments and based on available studies of butterfly-web bridges [1],[2] where web segment behaviour was described as an approximation with tensile and compressive diagonal. More suitable seems the analogy with a Vierendeel beam. Wall segments are thus approximated as frame members and their action is bending in longitudinal direction. Given the excellent UHPC properties in tensile strength in bending, this behaviour is most convenient.

6. CONCLUSIONS

In this paper the results were presented of an experimental analysis of UHPC beams with lightened webs and numerical verification in the program SCIA Engineer. These specimens demonstrate on a smaller scale the behaviour of precast web segments of a bridge with box cross-section, which are connected to the top and bottom monolithic slabs of the cross-section by composite action. Discrete behaviour of the web segments was compared to the continuous behaviour of a beam with solid web with constant thickness. The conclusion of the analysis is viability of application of UHPC precast webs especially due to the excellent properties of the UHPC in tension under bending action. When these web segments are provided with efficient prestressing to eliminate tensile stresses on their edges, the precast web segments provide superior performance compared to beams with a continuous web.

ACKNOWLEDGEMENTS

This work was supported by SGS grant of CTU in Prague, Czech Republic, grant No. SGS20/042/OHK1/1T/11.

References

Kasuga, N. Nagamoto, K. Kata, H. Asai (2010), Study of a bridge with a new structural system using ultra high strength fiber reinforced concrete, *Proceedings of 3nd fib Congress, Washington*

K. Kata, K., Ashizuka, K., Miyamoto, K., Nakatsumi, K., (2013), Design and Construction of Butterfly Web Bridge, *Third International Conference on Sustainable Construction Materials and Technologies, Kyoto.*

Fehling, E., Schmidt, M., Walraven, J., Leutbecher, T., Frohlich, S. Ultra-High Performance Concrete UHPC. *Berlin: Wilhelm Ernst & Sohn, Verlag für Architektur und technische Wissenschaften GmbH & Co. KG, 2014. ISBN 978-3-433-03087-5.*

Mazars J.;A description of micro and macroscale damage of concrete structure. *Eng Fract Mech 25:729–737,1986*

Němec I. Trcala M. Rek V; Nelineární mechanika, (Vutium, Brno, 2018)

Kupfer H., Hilsdorf H.K, Rusch H.: Behaviour of concrete under biaxial stresses, *ACI Journal, Title 66-52, 1969*

Wu J.Y., Li J., Faria R.: An energy release rate-based plastic-damage model for concrete, *International Journal of Solids and Structures, Volume 43, Issues 3–4, February 2006, Pages 583-612*